



Research on Wind Pressure Characteristics of Tall Building Claddings

Tao Ye^{1,2*}

¹Guangzhou Institute of Science and Technology, Guangzhou, 510540, China

²Department of Bridge Engineering, Tongji University, Shanghai, 200092, China

*Correspondence addressed: yetao1982827@163.com

Abstract. The fluctuating wind pressure in local areas of high-rise buildings exhibits strong volatility, which is affected by airflow separation and vortex shedding, making its probability distribution no longer conform to Gaussian distribution. This article takes the wind pressure test data of Shanghai Global Financial Center as the object, explores the statistical characteristics and probability distribution characteristics of fluctuating wind pressure, and provides conclusions. The research results indicate that for positive wind pressure, both normal distribution and Gamma distribution can well describe its distribution, followed by Weibull distribution. For the negative pressure in the separation zone, Gamma distribution and Weibull distribution can well describe its non-Gaussian distribution characteristics. For the negative pressure in the wake region, Gamma distribution and Weibull distribution can well describe its left tail distribution, while normal distribution can better describe its right tail distribution.

Keywords: High-rise building; Rigid body model; Fluctuating wind pressure distribution; Probability distribution characteristics; Non-Gaussian wind pressure

1 Introduction

The wind load acting on buildings is a random load, and there are generally two methods to determine the magnitude of the wind load to ensure the safety and economic design of the structure and maintenance components: one is to use the traditional probability guarantee method; The second is to use the extremum method to determine the extremum of wind pressure, which was originally introduced into wind engineering by Davenport^[1-4]. At present, research on the non-Gaussian characteristics of wind pressure is mostly focused on large-span roofs and low rise building roofs, with less attention paid to the probability characteristics of surface wind pressure in super high-rise buildings. Sun Ying et al.^[5-8] studied the non-Gaussian statistical characteristics of fluctuating wind pressure on the surface of large-span flat roofs, and explained the reasons for the non-Gaussian characteristics through the time and spatial correlation of wind pressure, combined with the central limit theorem. The fluctuating wind pressure in local areas of high-rise buildings exhibits strong volatility, which is affected by airflow separation and vortex shedding, causing its probability distribution to no longer follow

a Gaussian distribution. This article takes the wind pressure test data of Shanghai World Financial Center as the object, explores the statistical characteristics, probability distribution characteristics, and time-frequency domain characteristics of fluctuating wind pressure, analyzes and studies the extreme values of wind pressure, and provides conclusions.

2 Wind Pressure Characteristics of Tall Buildings

The classical extreme value theory (Fisher&Tippett 1928)^[9-14] holds that no matter what distribution a random variable satisfies, the maximum (extreme value) of a large number of independent identically distributed random variables will approximately obey any of the three extreme value distribution forms (extreme value I, II, III). Gumbel (1954)^[15-20] made a systematic study on this, and found that as long as the parent distribution follows the exponential distribution form (such as Gaussian distribution, Gamma distribution, Weibull distribution, etc.), the extreme value distribution of a large number of independent random variables will follow the extreme value I distribution (Gumbel distribution).

$$F(x) = e^{-e^{\left(\frac{x-b}{a}\right)}} \tag{1}$$

Its probability density function can be written as:

$$f(x) = \frac{1}{a} e^{\left[\frac{x-b}{a} - e^{\left(\frac{x-b}{a}\right)}\right]} \tag{2}$$

Where, a are scale parameters, and $a > 0$; b is the location parameter.

The surface wind pressure distribution of high-rise buildings follows a non-Gaussian distribution, which is further subdivided into various types, including Gamma distribution, Weibull distribution, etc. Several basic probability distribution expressions are as follows:

If the probability density function of random variable X satisfies the following formula:

$$f(x) = \frac{\left(\frac{x-\mu}{\beta}\right)^{\gamma-1} e^{-\frac{x-\mu}{\beta}}}{\beta\Gamma(\gamma)}, \quad x > \mu \tag{3}$$

The random variable is said to obey the gamma distribution, where μ, β, γ are the location parameters, scale parameters and shape parameters of the probability distribution, and $\Gamma(\cdot)$ is the gamma function $\Gamma(a) = \int_0^\infty e^{-t} t^{a-1} dt$.

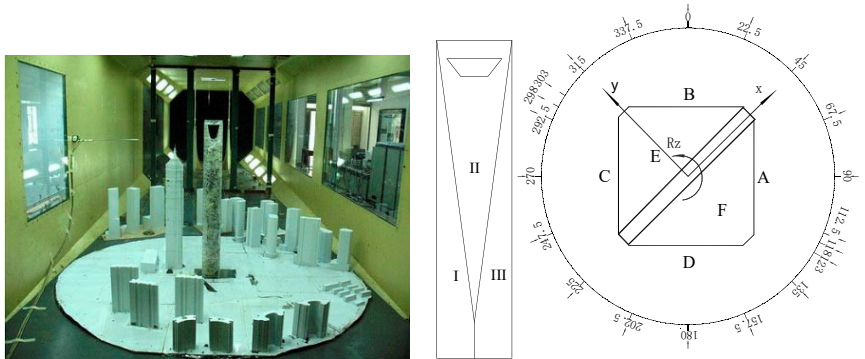
If the probability density function of random variable X satisfies the following formula:

$$f(x) = \frac{\gamma}{\beta} \left(\frac{x}{\beta}\right)^{\gamma-1} e^{-\left(\frac{x}{\beta}\right)^\gamma}, \quad 0 \leq x < \infty, \gamma > 0, \beta > 0 \tag{4}$$

The random variable is said to obey Weibull distribution, where γ, β are the shape parameters and scale parameters of the distribution respectively.

3 Research Methods of Wind Tunnel Test

This study takes the Shanghai World Financial Center as the engineering background and conducts rigid body model pressure measurement tests in the TJ-2 boundary layer wind tunnel of Tongji University. Turbulent field simulation for Class C site. Each pressure signal contains 6000 data points, with a sampling frequency of 312.5 Hz and a duration of 19.2 seconds. The total height of the model is 1.4 meters, with a scale ratio of 1:350. In this test, the reference wind speed is 14 meters per second, and monitoring is conducted at a height of 1.2 meters in the wind tunnel.



(a) Model test of rigid body pressure measurement (0° Wind direction angle)

(b) Definition of model orientation, elevation, wind direction and coordinate axis

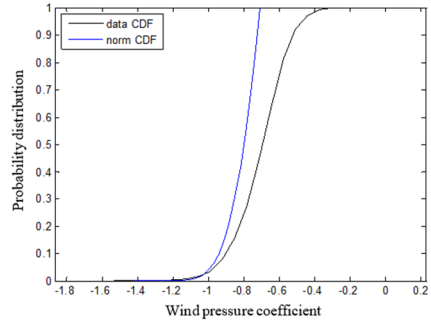
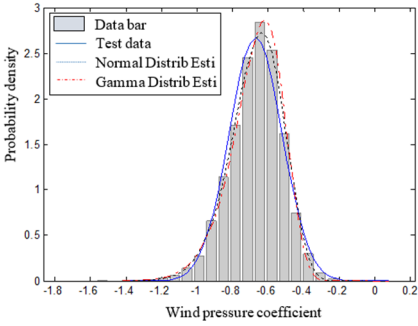
Fig. 1. Setup, facade, wind direction, and coordinate axis of the rigid model

4 Experimental Results and Analysis

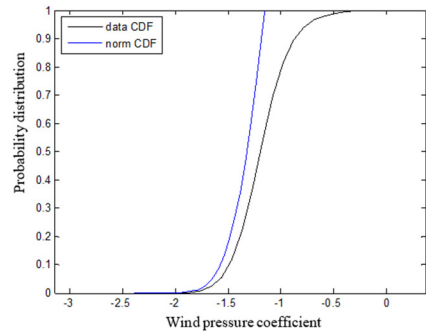
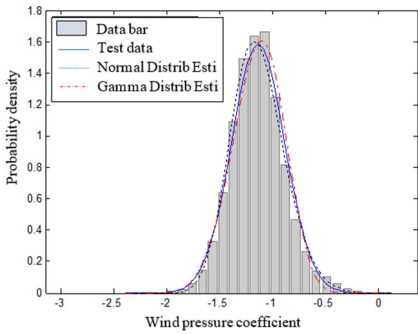
The rigid model pressure test is carried out according to 20 wind directions as shown in Figure 1. The wind direction angle ranges from $0^\circ \sim 360^\circ$ with an interval of 22.5° . In addition, four wind direction angles of 118° , 123° , 298° and 303° are added. The surrounding environment of the test is considered as a single global financial center (without any surrounding buildings), and the following experimental results are obtained under this experimental condition.

Figure 2 is the time history and probability density diagram of wind pressure coefficient of selected typical measuring points under different wind direction angles. Figure 2 (a) and (c) are the time history diagram and probability density diagram of wind pressure coefficient of windward side measurement points 28-39. Since the incoming flow on windward side is not disturbed, the fluctuating wind pressure meets the assumption of Gaussian distribution, and the actual distribution conforms well to the normal distribution; However, when the measuring point is on the crosswind plane (Figure 2 (b) and (d)), the measuring point is in the separation area, showing a long burr in the time history diagram, and the fluctuating wind pressure no longer obeys the Gaussian distribution; When the measuring point is on the leeward side (Figure 2 (e) and (g)), the fluctuating wind pressure can still be approximately described by Gaussian distribution, but

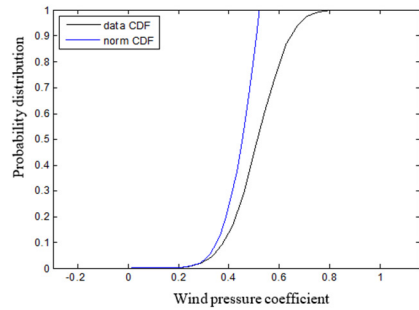
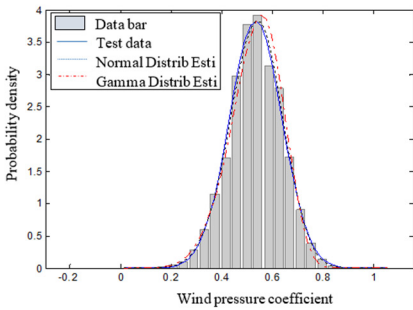
it shows great pulsation due to the influence of wake vortex. Figure 2 (f) and (h) reflect the non-Gaussian characteristics of wind pressure at measuring point 5-3 in the cross-wind area.



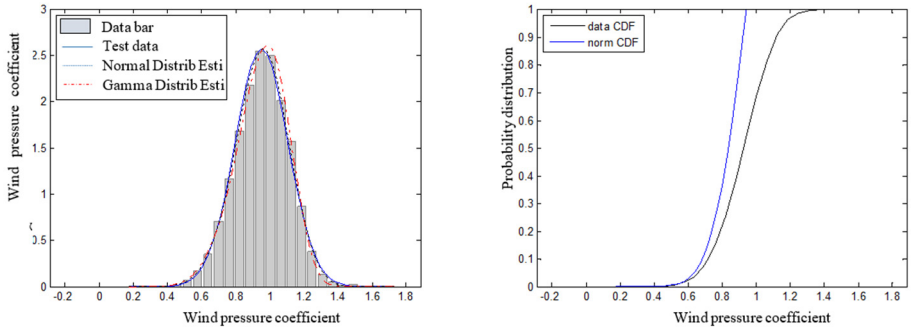
(a) Statistical characteristics of fluctuating wind pressure at measuring point 28-39 at 0° wind direction angle



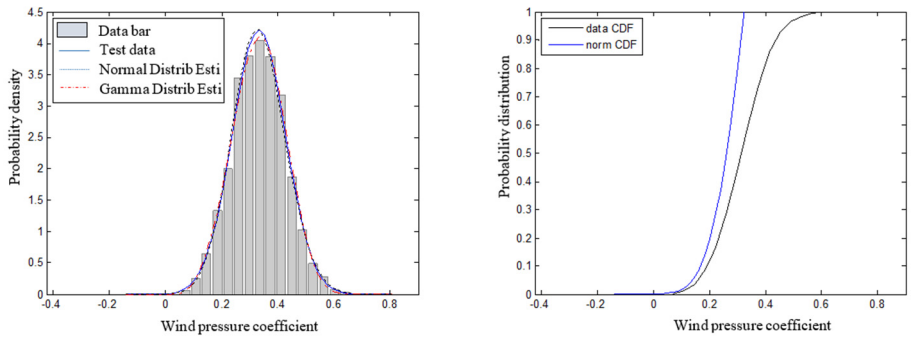
(b) Statistical characteristics of fluctuating wind pressure at measuring point 28-39 at 45° wind direction angle



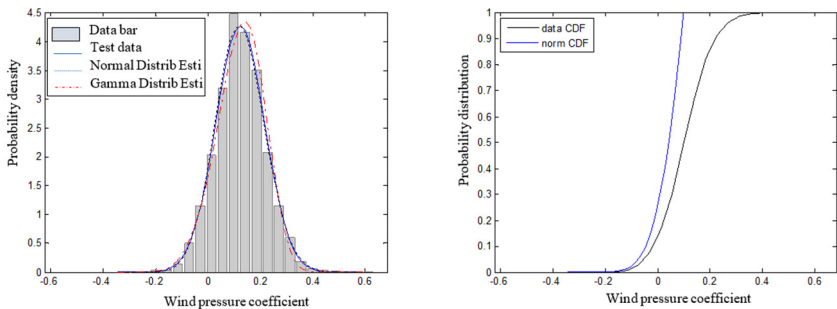
(c) Statistical characteristics of fluctuating wind pressure at measuring point 28-39 at 90° wind direction angle



(d) Statistical characteristics of fluctuating wind pressure at measuring point 28-39 at 135° wind direction angle



(e) Statistical characteristics of fluctuating wind pressure at measuring point 28-39 at 180° wind direction angle

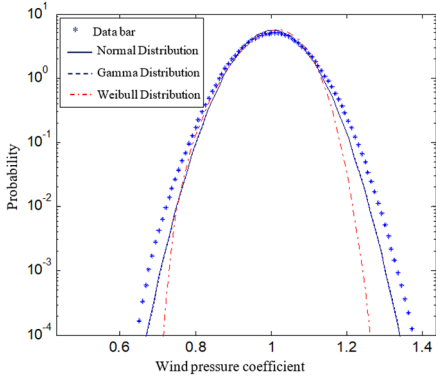


(f) Statistical characteristics of fluctuating wind pressure at measuring point 5-3 at 90° wind direction angle

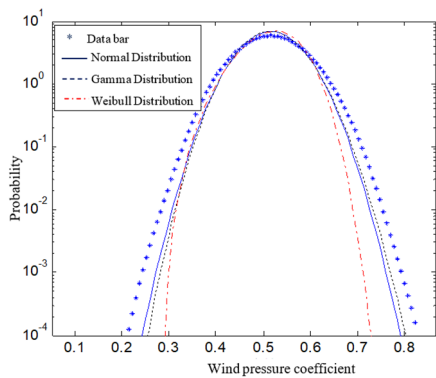
Fig. 2. Time history diagram of wind pressure coefficient at typical measurement points and corresponding probability density, probability distribution diagram

The tail of the wind pressure probability distribution directly affects the calculation of the wind pressure extreme value. In order to more clearly see the fitting of the tail of the wind pressure probability distribution, the ordinate probability density is set as the logarithmic coordinate system. See Figure 3 for the detailed fitting of the wind pressure probability distribution.

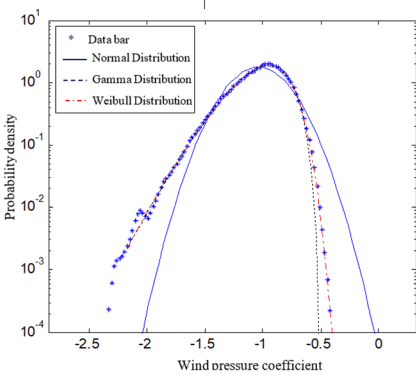
Figure 3 (a), (b), (f), and (g) indicate that in the positive wind pressure region, the fluctuating wind pressure conforms well to the Gaussian distribution, and its probability distribution can be well described by the normal distribution and Gamma distribution. However, the Weibull distribution provides a relatively poor description of these positive wind pressure probability distributions. Upon careful observation of Figure 3 (d), (e), (i), and (j), it can be seen that the Gamma and Weibull distributions can well describe the left tail distribution of wind pressure at these measurement points located in the wake region, while the normal distribution can better describe the right tail distribution.



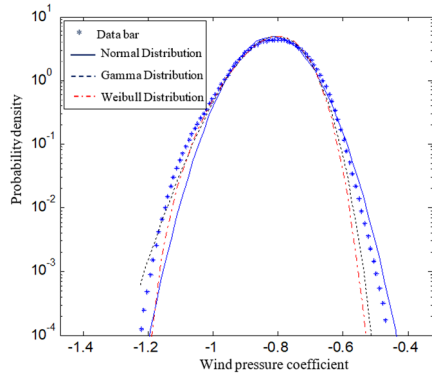
(a) Comparison of three distributions at measuring point 28-39 at 0° wind direction angle



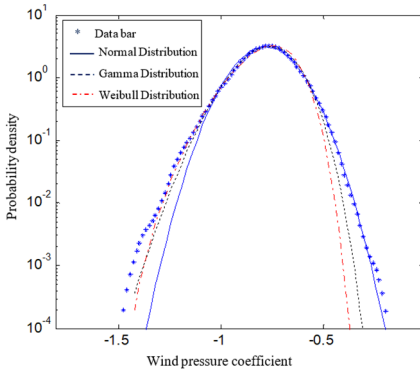
(b) Comparison of three distributions at measuring point 28-39 at 45° wind direction angle



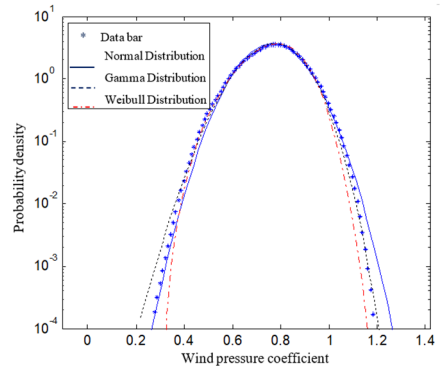
(c) Comparison of three distributions at measuring point 28-39 at 90° wind direction angle



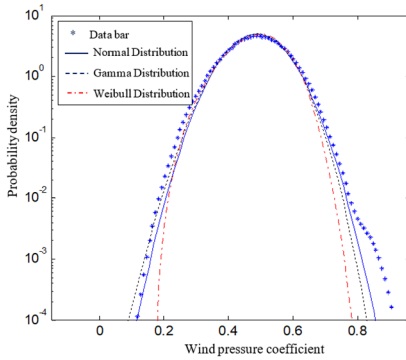
(d) Comparison of three distributions at measuring point 28-39 at 135° wind direction angle



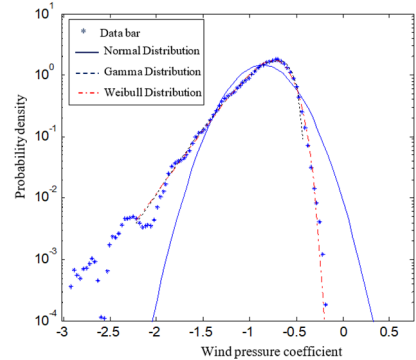
(e) Comparison of three distributions at measuring point 28-39 at 180° wind direction angle



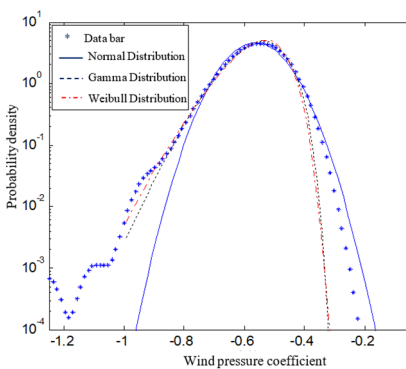
(f) Comparison of three distributions at measuring point 5-3 at 45° wind direction angle



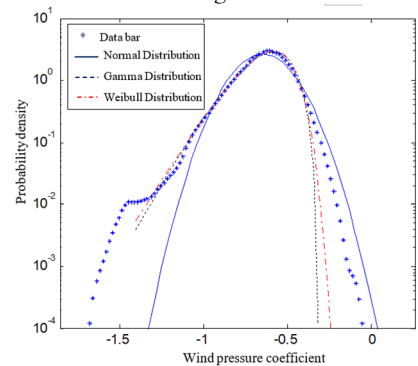
(g) Comparison of three distributions at measuring point 5-3 at 90° wind direction angle



(h) Comparison of three distributions at measuring point 5-3 at 135° wind direction angle



(i) Comparison of three distributions at measuring point 5-3 at 180° wind direction angle



(j) Comparison of three distributions at measuring point 5-3 at 225° wind direction angle

Fig. 3. Comparison of probability density fitting diagrams for typical distribution of wind pressure coefficients at typical measurement points

5 Conclusions

(1) The probability density distribution of non-Gaussian wind pressure on building surfaces cannot be uniformly and well fitted using existing mathematical models. For positive wind pressure, both normal distribution and Gamma distribution can describe its distribution well (in fact, when the shape parameter of Gamma distribution is large, Gamma distribution is very close to normal distribution), followed by Weibull distribution.

(2) For the negative pressure in the separation zone, Gamma distribution and Weibull distribution can well describe its non-Gaussian distribution characteristics.

(3) For the negative pressure in the wake region, Gamma distribution and Weibull distribution can well describe its left tail distribution, while normal distribution can better describe its right tail distribution.

Reference

1. Davenport A G. Note on the distribution of the largest value of a random function with application to gust loading[J]. Proc. of the Inst. of Civ. Engrs. , 1964,28: 187-196.
2. F.B. Chen, H.M. Liu, et al. Characterizing wind pressure on CAARC standard tall building with various façade appurtenances: An experimental study. Journal of Building Engineering,2022, 59(1): 1-10.
3. X.L. Han, Q.S. Li, et al. Comparative study between field measurements of wind pressures on a 600-m-high skyscraper during Super Typhoon Mangkhut and wind tunnel test. Engineering Structures,2022 (272),1-22.
4. D.M. Huang, G.L. Chen, et al. Wind pressure distribution, non-Gaussian characteristics, and conical vortices of a large-span roof with variable arc angles. Journal of Building Engineering. Journal of Building Engineering, vol.57(1), October 2022, 104929
5. Sun Ying, Wu Yue, Lin Zhixing, etc Non Gaussian characteristics of wind pressure pulsation in large-span roof structures [J]. Journal of Civil Engineering, 2007, 40 (4): 1-5.
6. Y. Li et al. Machine learning based algorithms for wind pressure prediction of high-rise buildings. Advances in Structural Engineering, vol.25(10), 2022.
7. Wind pressure distribution, non-Gaussian characteristics, and conical vortices of a large-span roof with variable arc angles Dongmei Huang a,b,* , Guoliang Chen. Journal of Building Engineering. Journal of Building Engineering, vol.57, 1 October 2022, 104929.
8. Dongmei Huang*, Zhaokun Zhu, Hongling Xie. Peak Factor Deviation Ratio Method for Division of Gaussian and Non-Gaussian Wind Pressures on High-Rise Buildings [J]. Mathematical Problems in Engineering, 2022.
9. Y.L. Xu, T.T. Liu, W S ZHANG. Buffeting. Induced Fatigue Damage Assessment of a Long Suspension Bridge. International Journal of Fatigue.2009. 31 (3):575-586.
10. Dongmei Huang*, Hongling Xie, Qiusheng Li*.A revised Hermite peak factor model for non-Gaussian wind pressures on high-rise buildings and comparison of methods [J]. 2023,36(1):15-29.
11. Hu W, Peng L, Yang Q, Liu L, Zhang P, Li S. Non-stationary characteristics and evolutionary power spectral density model of strong winds [J]. Authorea Preprints, 2023.
12. Yang Qingshan, Dan Wenshan, Tamura Yukio, Jin Rongche Characteristics of pulsating wind loads on high-rise buildings [J]. Journal of Civil Engineering, 2023, 56 (05): 1-17+88

13. Shen H, Hu W, Yang Q, Yang F, Guo K, Zhou T, Qian G, Xu Q, Yuan Z. Non-Gaussian wind features over complex terrain under atmospheric turbulent boundary layers: A case study[J]. *Wind and Structures*, 2022, 35(6): 419-430.
14. Chen B, Bian R, Chen Z, Wang X, Yang Q. Peak wind pressures on roof claddings of regular railway stations[J]. *Engineering Structures*, 2022, 259: 114178.
15. Cochran L S. Wind-tunnel modelling of low-rise structures: [J]Colorado State University, 1992.
16. Huang Mingfeng, Wang Chunhe, Lin Wei, Xiao Zhibin. 2022. Optimization of wind resistance performance design for super high-rise buildings based on optimization criteria particle swarm algorithm [J] *Journal of Architectural Structures*.
17. Zekang Wang, Xiaohong Wang, Heng Zhao, Bo Chen*, Qingshan Yang. Equivalent static wind loads on canopies of regular railway stations. *Engineering Structures*, 2023, 276, 115336
18. Kun Du, Bo Chen*. A hybrid semi-supervised regression based machine learning method for predicting peak wind loads on a group of buildings. *Engineering Structures*, 2023, 275, 115245
19. Bo Chen*, Rongfeng Bian, Zhuolun Chen, Xiaohong Wang, Qingshan Yang, Peak wind pressures on roof claddings of regular railway stations. *Engineering Structures*, 2022, 259, 114178
20. He Bin; Quan yong; Gu Ming Wind direction reduction factor for the design wind speed of high-rise buildings under a deviated wind field [J] *Journal of Tongji University (Natural Science Edition)*, June 4, 2024.

Open Access This chapter is licensed under the terms of the Creative Commons Attribution-NonCommercial 4.0 International License (<http://creativecommons.org/licenses/by-nc/4.0/>), which permits any noncommercial use, sharing, adaptation, distribution and reproduction in any medium or format, as long as you give appropriate credit to the original author(s) and the source, provide a link to the Creative Commons license and indicate if changes were made.

The images or other third party material in this chapter are included in the chapter's Creative Commons license, unless indicated otherwise in a credit line to the material. If material is not included in the chapter's Creative Commons license and your intended use is not permitted by statutory regulation or exceeds the permitted use, you will need to obtain permission directly from the copyright holder.

